Crystal Orientation and Thickness Dependence of the Superconducting Transition Temperature of Tetragonal FeSe$_{1-x}$ Thin Films

M. J. Wang,[1,*] J. Y. Luo,[2] T. W. Huang,[2] H. H. Chang,[3] T. K. Chen,[2] F. C. Hsu,[1] C. T. Wu,[3] P. M. Wu,[4]
A. M. Chang,[4] and M. K. Wu[2,3,†]

[1]*Institute of Astronomy and Astrophysics, Academia Sinica, Taipei, Taiwan*
[2]*Institute of Physics, Academia Sinica, Nankang, Taipei, Taiwan*
[3]*Department of Physics, National Tsing Hua University, Hsinchu, Taiwan*
[4]*Department of Physics, Duke University, Durham, North Carolina, USA*

(Received 9 April 2009; published 10 September 2009)

Superconductivity was recently found in the tetragonal phase FeSe. A structural transformation from tetragonal to orthorhombic (or monoclinic, depending on point of view) was observed at low temperature, but was not accompanied by a magnetic ordering as commonly occurs in the parent compounds of FeAs-based superconductors. Here, we report the correlation between structural distortion and superconductivity in FeSe$_{1-x}$ thin films with different preferred growth orientations. The films with preferred growth along the c axis show a strong thickness dependent suppression of superconductivity and low temperature structural distortion. In contrast, both properties are less affected in the films with (101) preferred orientation. These results suggest that the low temperature structural distortion is closely associated with the superconductivity of this material.

DOI: 10.1103/PhysRevLett.103.117002 PACS numbers: 74.62.Bf, 74.70.Ad, 74.78.Db

Superconductivity was recently discovered in tetragonal FeSe$_{1-x}$ with transition temperature $T_C \sim 8$ K [1]. Partially substituting relatively larger Te ion on the Se sites was found to enhance the superconducting transition temperature T_C [2,3]. It was also found that the application of high pressure can further increase the T_C to $\sim$39 K [4]. More detailed studies of this system, which has the simplest Fe planar structure, may provide critical information to better understand the origin of superconductivity in the Fe-based superconductors. Early muon spin rotation and NMR experiments [5,6] suggested that FeSe$_{1-x}$ is an unconventional superconductor. A more recent detailed NMR study [7] pointed out that superconductivity in FeSe$_{1-x}$ might have similar origin as that of the electron-doped Fe-pnictide superconductors. However, it is noted that a low temperature structural distortion was observed in FeSe$_{1-x}$ superconductors [1,8] without accompanying a magnetic ordering. This observation appears quite different from the Fe-pnictide superconductors. In the parent compounds of the Fe-pnictide superconductor, there exists a magnetic order, which comes with the low temperature tetragonal to orthorhombic structural transformation [9,10]. The structural transformation and magnetic ordering are suppressed with increasing doping, and subsequently, superconductivity appears. Wu *et al.* have reported the suppression of the superconductivity in Cu-substituted (Fe$_{1-x}$Cu$_x$)Se$_{1-x}$ samples [11]. It was also observed that there was no low temperature structural distortion in the nonsuperconducting (Fe$_{1-x}$Cu$_x$)Se$_{1-x}$ samples. This correlation suggested that the low temperature structural distortion might be essential for the occurrence of superconductivity. It is therefore important to establish the correlation between the occurrence of superconductivity and a low temperature structural distortion with pure and high quality FeSe$_{1-x}$ samples. Here, we report the observation in FeSe$_{1-x}$ thin films that the superconductivity exhibits strong orientation and film thickness dependence, which suggests that the occurrence of superconductivity in FeSe$_{1-x}$ is closely correlated with a low temperature lattice distortion.

The superconducting tetragonal FeSe$_{1-x}$ thin films on (001) MgO substrates were grown using a pulsed laser deposition (PLD) technique [11]. The structures of deposited films were first characterized by an x-ray diffractometer. Detailed structure analysis at low temperature was performed using 4-circle x-ray diffractometer with incident beam (12.4 keV) at BL13A in NSRRC and BL12B2 in Spring8. High resolution transmission electron microscope (HRTEM) and scanning transmission electron microscope/energy dispersive x-ray analysis (STEM/EDX) were also used to determine the film characteristic at the interface and the composition homogeneity, respectively. The temperature dependence of resistivity was characterized in a Quantum Design physical property measurement system (QD-PPMS).

We prepared FeSe$_{1-x}$ thin films on (001) MgO substrate at various temperatures. We present here only those films with the substrate temperature set at 320 °C (hereafter we designate these as LT-FeSe films) and 500 °C (hereafter, we designate these as HT-FeSe films). Figure 1(a) shows the x-ray diffraction patterns for LT-FeSe and HT-FeSe films, respectively. The thicknesses of both films are estimated to be $\sim$140 nm. We observed in the LT-FeSe sample only (001) peaks of the tetragonal phase FeSe$_{1-x}$, suggest-

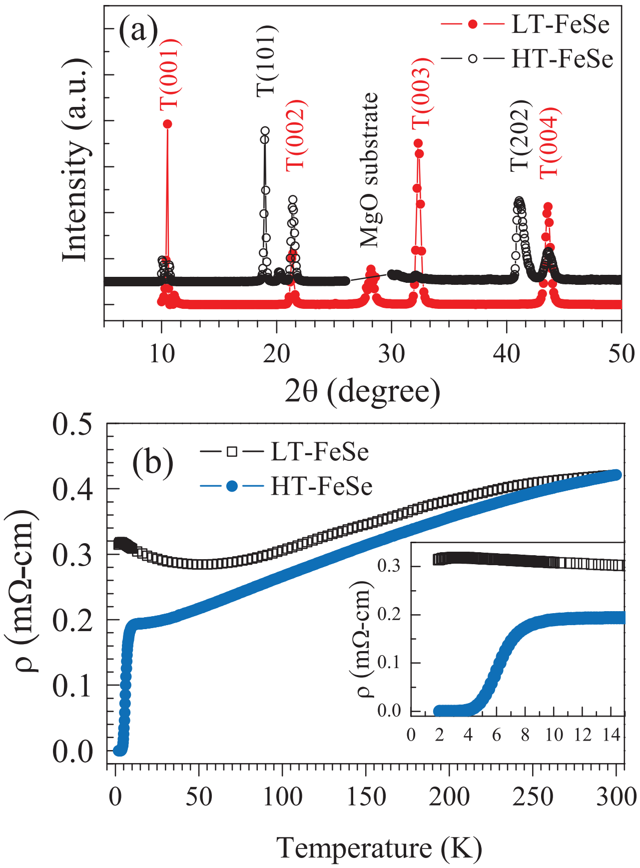

FIG. 1 (color). (a) The x-ray diffraction pattern of LT- and HT-FeSe_{1-x} films. At higher growth temperature, the intensity of (00l) peaks weakens while the (101) peak intensity becomes stronger. (b) The ρ-T curves of LT- and HT-FeSe_{1-x} films grown at different substrate temperature. At higher growth temperature, the ρ-T behavior is more metallic-like, and a clear superconducting transition is observed only for HT-FeSe. The inset is a close-up of the ρ-T below 15 K.

ing strong c-axis preferred orientation. However, the HT-FeSe film shows the (101) peaks to be dominant. Figure 1(b) displays the ρ-T curves of the LT-FeSe and HT-FeSe films, respectively. It is surprising to observe that the LT-FeSe film exhibits only a slightly resistive drop at 2 K without a complete superconducting transition. On the contrary, a clear superconducting transition takes place in the HT-FeSe films. The superconductivity is strongly correlated to the growth orientation of the films.

Detailed transmission electron micrographs for the HT- and LT-FeSe films are shown in Fig. 2. The film growth direction is along (101) for the HT-FeSe in (a) and (001) for LT-FeSe in (b), revealed by the selected-area electron diffraction (SAED) patterns as shown in the insets. The SAED patterns indicate that both films are well-aligned with MgO substrates. However, a transition layer around 3 to 6 nm was found in (a) while a much thinner ($\leq$1 nm) transition layer is in (b).

The suppression of superconductivity for the LT-FeSe thin film was puzzling, particularly since the samples

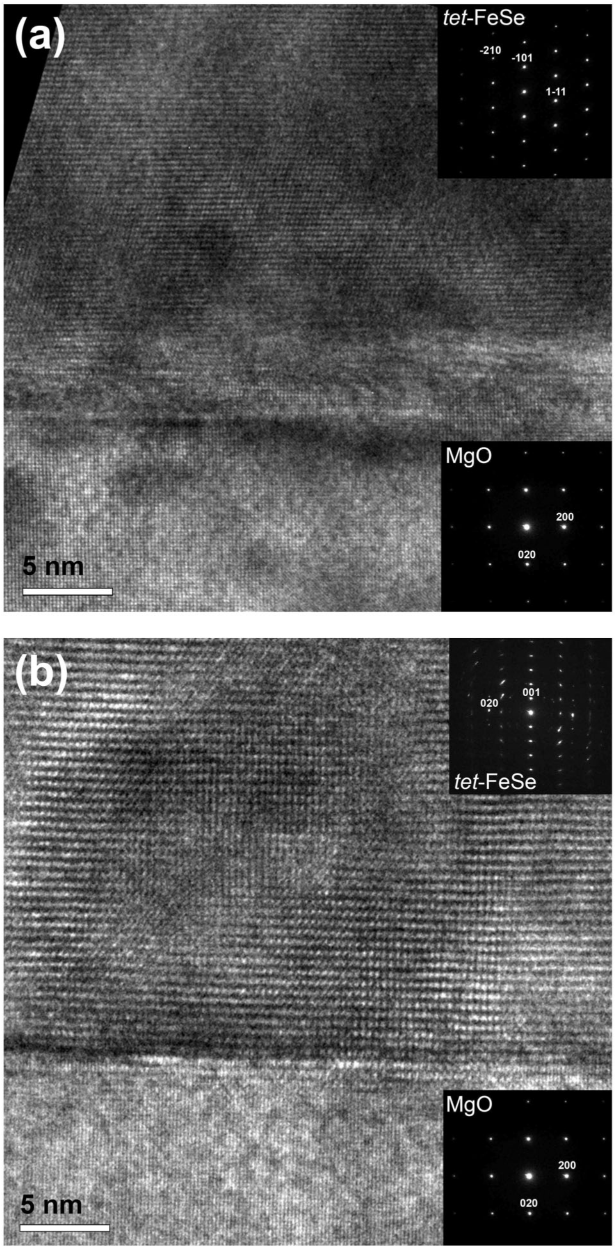

FIG. 2. Cross section TEM images of (a) 1 μm (HT-)FeSe thin films. The film growth direction is along (101), revealed by the SAED patterns (top right inset). (b) (LT-)FeSe thin films. The film growth direction is along (001), revealed by the SAED patterns (top right inset).

showed pure tetragonal phase with nearly epitaxial growth on the substrate. We next prepared a series of LT- and HT-FeSe with different film thickness. Figure 3(a) shows the resistive superconducting transition of LT-FeSe films with thickness ranging from 140 nm to 1 μm. As the film is made thicker, the onset T_C of film recovers more closely to the bulk result, as shown in the inset of Fig. 3(a). On the other hand, the HT-FeSe film does not exhibit significant film thickness dependence, as shown in Fig. 3(b) and inset. The superconducting transition temperatures for HT-FeSe films are close to the bulk sample value.

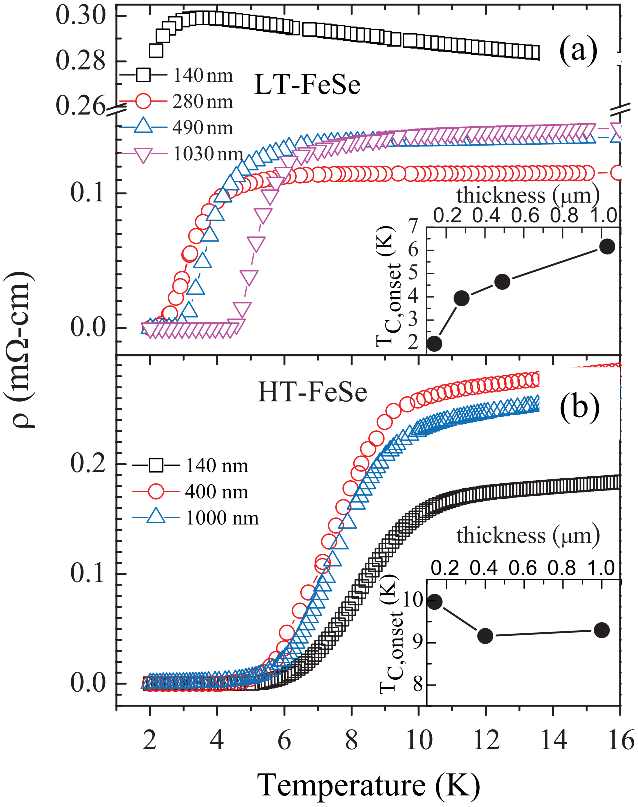

FIG. 3 (color). (a) The ρ-T curves of LT-FeSe films with thickness from 140 to 1030 nm. The inset shows the strong thickness dependence of onset T_C. As the film is made thicker, T_C approaches the bulk result. (b) The ρ-T curves of HT-FeSe films with different thickness. The onset T_C shows less thickness dependence, shown in the inset.

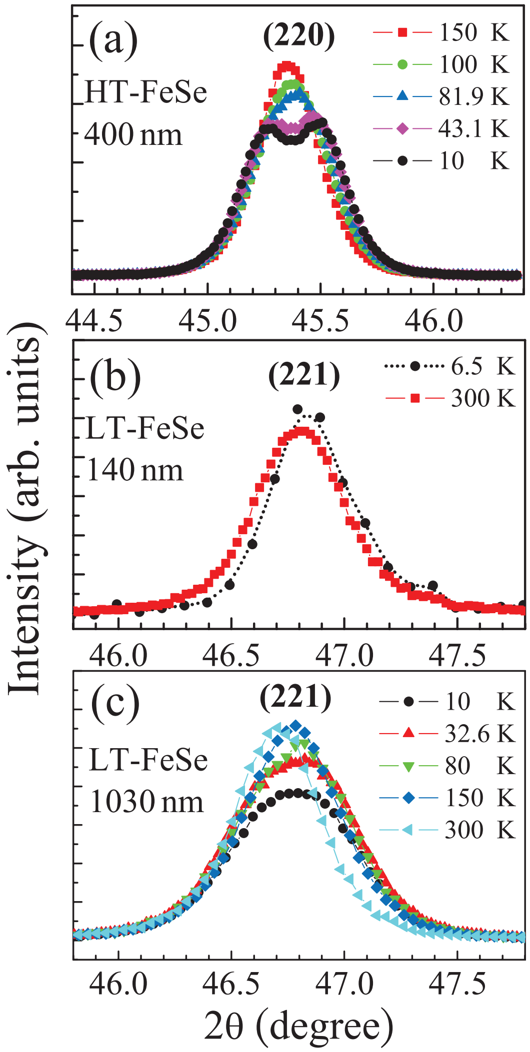

FIG. 4 (color). (a) The x-ray diffraction (220) peaks of HT-FeSe film at different temperatures. The results show the splitting of the Bragg peak indicating a structural distortion occurs at around 82 K. The x-ray diffraction pattern of LT-FeSe films for (b) 140 and (c) 1030 nm film at different temperatures. The data show that for 140 nm film, the (221) Bragg peak does not change with temperature; for 1030 nm film, the (221) peak becomes broadened at low temperature.

To better understand the observed behavior, we examined several factors. The possibility that the superconductivity disappearing in thin LT-FeSe films, but reappearing in thicker films, is due to the presence of Se-content gradient on the film can be ruled out from the detailed STEM/EDX mappings (shown in supplementary information [12]) of the 1 μm thick LT-FeSe film. The Fe and Se concentrations were found uniformly distributed along the growth direction, out of substrate plane. Another possibility is the strain effect from the interface because of the lattice mismatch between the thin film and the substrate, which could extend or compress the lattice constants. This may subsequently affect the physical properties of the film, especially for thinner ones. However, the lattice constants derived from the high resolution x-ray diffraction of the sample are found very close to the values of the bulk in both LT- and HT-FeSe samples, $a = 3.78$ Å and $c = 5.54$ Å at room temperature. Thus, it is unlikely for the lattice mismatch to be the dominant cause for the observed strong thickness dependence of superconductivity in the LT-FeSe.

This unusual observation led us to investigate in detail whether the low temperature structural distortion observed in the superconducting FeSe could be the cause of such unusual film thickness dependence. Figure 4(a) is the x-ray diffraction (220) peaks at different temperatures of the superconducting HT-FeSe film (thickness ~400 nm). The results clearly show the splitting of (220) peak confirming the presence of a structural distortion as reported in bulk samples [1,8], which occurs around 82 K. Thus, the lattice strain due to lattice mismatch between the film and the substrate does not affect the structural distortion of HT-FeSe film at low temperature. On the other hand, the LT-FeSe film with 140 nm thickness, which is not superconducting, shows no structural distortion at low temperature as only one single peak appears in the x-ray diffraction pattern at high and low temperatures, Fig. 4(b). However, in the diffraction pattern of 1 μm superconducting film, the (221) diffraction peak gradually becomes broadened, and the maximum value is decreased as the temperature decreases to 10 K, as shown in Fig. 4(c). This indicates that in LT-FeSe thin film the low temperature structural distortion is suppressed by the interface effect, but this effect can be gradually released as film thickness increases.

These results can possibly be understood with the following picture. The LT-FeSe film, which exhibits (00l) preferred orientation, would experience stronger lattice strain effect so that the atoms in the FeSe a-b plane close to the film-substrate interface are pinned to the substrate atoms. Since the low temperature lattice distortion occurs within the a-b plane, the structural distortion in thinner LT-FeSe films is most likely suppressed by this lattice strain effect. This strain effect is gradually relaxed as the film thickness increases. In contrast, the lattice distortion in the HT-FeSe film is obviously not affected by the substrate strain effect because the film aligns preferably along (101) orientation.

These results strongly support the conjecture that the dependence of superconductivity on film thickness is associated with the ability of the lattice to undergo low temperature structural distortion, and further confirm the importance of the low temperature structural distortion to the origin of superconductivity in the FeSe system. Although the actual mechanism has yet to be identified, our results may provide an important clue to understand the origin of superconductivity in FeSe.

In summary, we have successfully deposited tetragonal FeSe_{1-x} films on (001) MgO substrates by the PLD technique. The deposited FeSe film has (001) and (101) preferred orientations when grown at 320 °C (LT-FeSe) and 500 °C (HT-FeSe), respectively. Strong thickness dependence of superconductivity is observed in the LT-FeSe films, but essentially no thickness dependence is observed in the HT-FeSe cases. The LT-FeSe films have a T_C much lower than that of HT-FeSe films which is close to the bulk value. Furthermore, high resolution x-ray diffraction shows the low temperature structural distortion of LT-FeSe films is strongly suppressed in thinner films and is recovered gradually for thicker films. On the contrary, both superconductivity and low temperature structural distortion are not affected in HT-FeSe films. Our results strongly indicate the correlation of the low temperature structural distortion to the occurrence of superconductivity in these FeSe thin films.

The authors acknowledge the support from the Taiwan National Synchrotron Radiation Research Center for the detailed low temperature x-ray diffraction. This work was partially supported by the Taiwan National Science Council and the US AFOSR grants.

Note added.—After we submitted our manuscript, a paper appeared [13] which also demonstrated that a low temperature structural distortion is observed in the superconducting $\text{Fe}_{1+\delta}\text{Se}$ ($\delta = 0.01$) samples, but not in the nonsuperconducting $\text{Fe}_{1+\delta}\text{Se}$ ($\delta = 0.03$) samples.

---

*mingjye@asiaa.sinica.edu.tw
†mkwu@phys.sinica.edu.tw

[1] F.-C. Hsu, J.-Y. Luo, K.-W. Yeh, T.-K. Chen, T.-W. Huang, P. M. Wu, Y.-C. Lee, Y.-L. Huang, Y.-Y. Chu, and D.-C. Yan *et al.*, Proc. Natl. Acad. Sci. U.S.A. **105**, 14262 (2008).

[2] K.-W. Yeh, T.-W. Huang, Y.-L. Huang, T.-K. Chen, F.-C. Hsu, P. M. Wu, Y.-C. Lee, Y.-Y. Chu, C.-L. Chen, and J.-Y. Luo *et al.*, Europhys. Lett. **84**, 37002 (2008).

[3] Y. Mizuguchi, F. Tomioka, S. Tsuda, T. Yamaguchi, and Y. Takano, J. Phys. Soc. Jpn. **78**, 074712 (2009).

[4] Y. Mizuguchi, F. Tomioka, S. Tsuda, T. Yamaguchi, and Y. Takano, Appl. Phys. Lett. **93**, 152505 (2008).

[5] R. Khasanov, K. Conder, E. Pomjakushina, A. Amato, C. Baines, Z. Bukowski, J. Karpinski, S. Katrych, H.-H. Klauss, and H. Luetkens *et al.*, Phys. Rev. B **78**, 220510 (2008).

[6] H. Kotegawa, S. Masaki, Y. Awai, H. Tou, Y. Mizuguchi, and Y. Takano, J. Phys. Soc. Jpn. **77**, 113703 (2008).

[7] T. Imai, K. Ahilan, F. L. Ning, T. M. McQueen, and R. J. Cava, Phys. Rev. Lett. **102**, 177005 (2009).

[8] S. Margadonna, Y. Takabayashi, M. T. McDonald, K. Kasperkiewicz, Y. Mizuguchi, Y. Takano, A. N. Fitch, E. Suard, and K. Prassides, Chem. Commun. (Cambridge) **43**, 5607 (2008).

[9] C. de la Cruz, Q. Huang, J. W. Lynn, J. Li, W. Ratcliff II, J. L. Zarestky, H. A. Mook, G. F. Chen, J. L. Luo, and N. L. Wang *et al.*, Nature (London) **453**, 899 (2008).

[10] Q. Huang, Y. Qiu, W. Bao, M. A. Green, J. W. Lynn, Y. C. Gasparovic, T. Wu, G. Wu, and X. H. Chen, Phys. Rev. Lett. **101**, 257003 (2008).

[11] M. K. Wu, F. C. Hsu, K. W. Yeh, T. W. Huang, J. Y. Luo, M. J. Wang, H. H. Chang, T. K. Chen, S. M. Rao, and B. H. Mok *et al.*, Physica C (Amsterdam) **469**, 340 (2009).

[12] See EPAPS Document No. E-PRLTAO-103-056938 for supplementary material. For more information on EPAPS, see http://www.aip.org/pubservs/epaps.html.

[13] T. M. McQueen, A. J. Williams, P. W. Stephens, J. Tao, Y. Zhu, V. Ksenofontov, F. Casper, C. Felser, and R. J. Cava, Phys. Rev. Lett. **103**, 057002 (2009).